International Journal of Rotating Machinery, 9(1): 41–47, 2003

1023-621X/03 $12.00 + .00
DOI: 10.1080/10236210390147371

Taylor & Francis
Taylor & Francis Group

Thermomechanical Behavior of Rotor with Rubbing

Jerzy T. Sawicki and Alberto Montilla-Bravo
Department of Mechanical Engineering, Cleveland State University, Cleveland, Ohio, USA

Zdzislaw Gosiewski
Aviation Institute, Warsaw, Poland

This article presents an analytical study of the dynamics and stability of rotors subjected to rubbing due to contact with seals, taking account of associated thermal effects. The seal interaction force acting on the shaft gives rise to a friction force, which is a source of heating and can induce so-called spiral vibrations. A mathematical model that has been developed couples the heat-conduction equation with the equations for motion of the rotor. Numerical simulations have been conducted that show the thermomechanical behavior of the rotor at various operating conditions. A procedure for analyzing the stability of multibearing rotors based on the system eigenvalue analysis and the state-space approach has been proposed. Finally, the experimental data related to full annular rub have been presented.

Keywords contact force, rotor rubbing, spiral vibration, stability, thermal bow

Steam turbine rotors are generally large, precision-machined steel forgings with multiple turbine wheels machined directly out of a single forging for the attachment of buckets (blades). Such rotors can exceed 20 feet in length and can have body diameters exceeding 30 inches. As such, most steam turbine rotors are relatively flexible as compared to gas turbine rotors that employ a bolted construction. Because of this, most steam turbine rotors operate at speeds exceeding the first critical speed and sometimes operate near their second critical speed. One consequence of the integral rotor design and the relative flexibility of the rotors is that steam turbine rotors can be sensitive to rub-induced vibrations. This is unfortunate, since steam turbines employ multiple turbine stages to extract energy from the steam and therefore require many seals between the static and rotating elements to minimize parasitic leakage and maximize thermal performance. Obviously, minimizing the rotor/seal clearances enhances thermal performance; the drawback to this approach is the increased risk of rotor/seal rubs and the resulting rotor vibration. This vibration may be self-correcting (stable), or self-propagating (unstable). In the worst case, the vibration can prohibit operation of the machine.

The rubbing phenomenon in rotating machinery has been widely written about during the past 3 decades. It has been well recognized that under certain conditions rotating machinery exhibits vibrations that have chaotic content, that is, they present unpredictable behavior. Such behavior is driven by the existence of nonlinearities in the system, which could have many roots; one of them is the interaction of the rotating and stationary components (Bently, 1974; Ehrich, 1992; Goldman and Muszynska, 1993, 1994; Kraker et al., 1988; Muszynska, 1989; Padovan and Choy, 1987). Numerous papers have employed bifurcation diagrams or Poincaré maps to report on the chaotic nature of rub interactions; for example, see Bently (1974), Goldman and Muszynska (1993), and Sawicki (1999). Some authors have explained the occurrence of such phenomena in terms of induced nonlinearities, for example, Sawicki (1999).

A relatively small number of papers have addressed the thermal effect associated with the rubbing of a rotor against its stationary components, which tends to heat the rotor at the angular location of the rub and is responsible for the rotor thermal balance change, known as the Newkirk effect. Based on Taylor's results (1924), Newkirk (1926) pointed out that when a rubbing rotor is running below its first balance resonance speed, the rub-induced lateral vibrations increase in time. Since then, many researchers have studied this effect. The most significant analyses have been provided by Dimarogonas (1973, 1983) and by Kellenberger (1980). Childs (1997) extended the Kellenberger model to include the effects of a radial clearance at the rub location. All these authors confirmed that these vibrations grow in amplitude and phase, resulting in spiral vibrations. One example is contacts between the rotor and seals, such as oil-lubricated

Received 20 March 2001; accepted 18 October 2001.
Address correspondence to Jerzy T. Sawicki, Department of Mechanical Engineering, Cleveland State University, Cleveland, OH 44115-2425, USA. E-mail: j.sawicki@csuohio.edu

generator shaft seals (Kellenberger, 1980) or brush seals (Sawicki, 2000), which can generate an asymmetrical peripheral temperature distribution and consequent rotor bow. If that is coupled with rotor vibration, a spiraling phenomenon may be observed. Another example is asymmetrical heating of the journal in fluid-film bearings; for example, see Kirk and Balbahadur (2000). The thermally induced vibrations can lead to problems, such as difficulties in performing proper balancing or, in serious cases, a situation in which it is impossible to operate the machine.

This article presents an analytical study of the dynamics of rotors subjected to rubbing due to contact with seals and also considers thermal effects. The induced thermal bow is modeled on Kellenberger's approach (1980). A mathematical model that has been developed couples the heat conduction equation with the equations of motion for the rotor. Numerical simulations that have been conducted show the thermomechanical behavior of the rotor at various operating conditions. The procedure for stability analysis of the multibearing rotor systems based on the eigenvalue analysis and state-space approach is proposed. Finally, the experimental data related to the full annular rub have been presented.

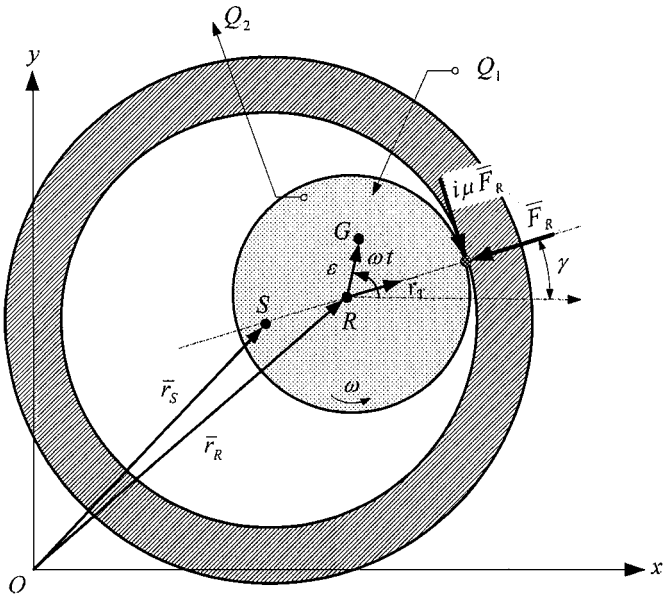

FIGURE 2
The rotor/stator interaction model.

ROTOR/STATOR CONTACT MODEL

The model of a rotor/stator system is shown in Figure 1, where the rotor is a Jeffcott (Laval) rotor—that is, uniform, massless, and having an elastic shaft carrying a rotor (disk) at its midspan. The bearings in this model are considered to be rigid and frictionless. The rotor has mass, m_R, stiffness, k_R, and damping, c_R. The stator has mass, m_S, and is mounted on a foundation via spring, k_S, and damper, c_S. The concentric radial clearance between the rotor and stator is C.

The kinematics of the rotor/stator contact model are illustrated in Figure 2. It is postulated that contact between the rotor and the stator takes place if the following condition is satisfied:

$$\delta = \delta^* - C = |\bar{r}_R - \bar{r}_S| - C > 0 \qquad [1]$$

where δ^* is the relative radial displacement of the rotor and stator, and δ is the penetration depth.

In addition, it is assumed that as a result of contact, the rotor/stator (contact) stiffness increases, and induced contact force, $\bar{F}_R$, is the result of nonlinear contact radial load and nonlinear tangential friction load, which are related by the Coulomb friction coefficient μ. A portion of heat generated by friction load Q_1 diffuses into the rotor, and the portion Q_2 diffuses out of the rotor. Also, it is assumed that if the contact condition in Equation (1) is satisfied, the induced contact force modeled by a simple model takes the form

$$\bar{F}_R = k_C \delta^n e^{i\alpha} \qquad [2]$$

where the contact stiffness k_C is a function of the material properties and geometry of the contacting components, and the coefficient of restitution is $n = 1.5$ for the Hertzian type of contact.

Following the notation in Figure 2, the nonlinear equations of motion for the rotor/stator system in complex vector notation $\bar{r} = x + iy$ are

$$\begin{cases} m_R \dfrac{d^2}{dt^2}(\bar{r}_R + \varepsilon e^{i\omega t}) + c_R \dot{\bar{r}}_R + k_R(\bar{r}_R - r_T e^{i\gamma}) = -(1 + i\mu)\bar{F}_R \\ m_S \ddot{\bar{r}}_S + c_S \dot{\bar{r}}_S + k_S \bar{r}_S = (1 + i\mu)\bar{F}_R \end{cases} \qquad [3]$$

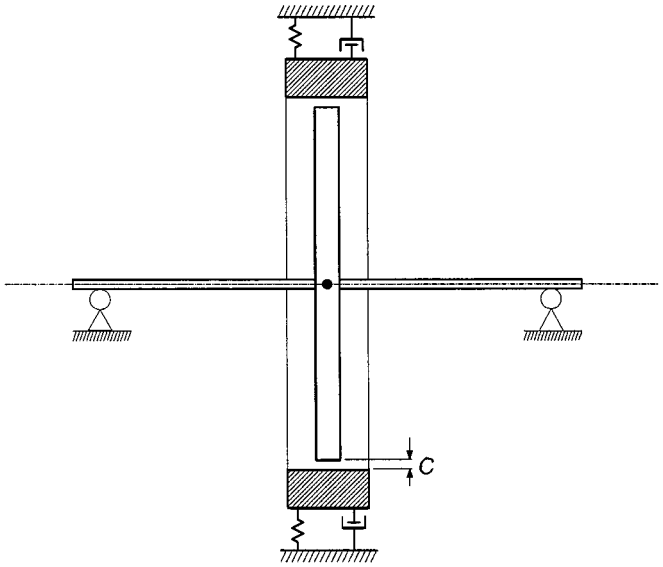

FIGURE 1
Schematic of rotor/stator model.

THERMAL BOW OF THE ROTOR

The radial contact force, $\bar{F}_R$, acting on the shaft (see Figure 2) gives rise to a friction force, which is a source of heating. Kellenberger (1980) used a heat-balance equation to arrive at the following definition for excess temperature T:

$$\dot{T}(t) = \frac{k_1}{k_3}\mu\omega R F_R(t) - \frac{k_2}{k_3}T(t) \qquad [4]$$

where

R is the rotor radius at which contact occurs;
F_R is the seal interactive force;
$\mu\omega R F_R(t)$ is the power dissipated due to rubbing contact;
k_1 is the proportionality factor defining the proportion of generated power that enters the shaft;
k_2 is the proportionality factor that defines the amount of heat lost from the shaft; and
k_3 is the factor that is proportional to the specific heat, density, and geometry of the shaft in the vicinity of the rubbing location.

Following Kellenberger's (1980) development, we assumed that the shaft's thermal deflection (bow) was proportional to the excess temperature, T, that is,

$$\rho_T = k_4 T \qquad [5]$$

where ρ_T is the rotating shaft with thermal deflection, and k_4 is the proportionality factor containing the thermal expansion coefficient, the material constants of the shaft, and the rotor's geometry, such as diameter, length, and bearings positions.

Now, taking into account the relationship in Equation (5), the temperature, Equation (4), can be rewritten in terms of thermal deflection in stationary coordinates as

$$\dot{\bar{r}}_T(t) - i\omega\bar{r}_T(t) + \hat{p}\mu\omega R\bar{F}_R(t) + \hat{q}\bar{r}_T(t) = 0 \qquad [6]$$

where parameters p and q characterize heat input and heat output, respectively, for the shaft and are defined as

$$\hat{p} = \frac{k_1 k_4}{k_3}, \quad \hat{q} = \frac{k_2}{k_3} \qquad [7]$$

Note that the rotor/stator's motion, Equation (3), and thermal bow, Equation (6), are coupled by the normal and tangential components of the contact force and by the thermal bow vector, $\bar{r}_T$. Equations (3) and (6) are written in inertial coordinates.

NUMERICAL RESULTS

The equations of motion, Equations (3) and (6), can be written in a nondimensional format by introducing the dimensionless time $z = \omega_R t$, and the following definitions (Kellenberger, 1980; Liebich, 1998):

$$\omega_R = \sqrt{\frac{k_R}{m_R}}, \; p = \hat{p}Rk_R, \; q = \frac{\hat{q}}{\omega_R}, \; \xi_R = \frac{c_R}{2m_R\omega_R}, \; \eta = \frac{\omega}{\omega_R} \qquad [8]$$

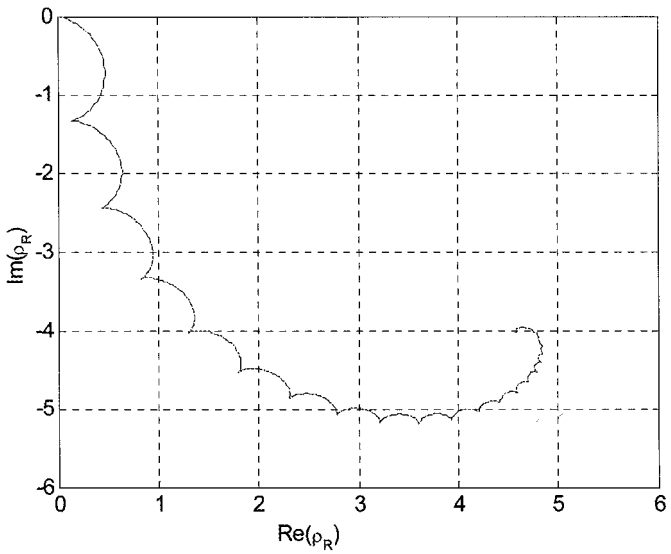

FIGURE 3
Rotor response, in rotating coordinates, to rub, without thermal effects. $\eta = 0.95$, $p = 0$, $q = 1 \times 10^{-3}$, $\xi_R = 0.05$, $M_S = 1 \times 10^{-5}$, $C_S = 0.7$, $K_S = 200$, $\mu = 0.2$, $K_C = 1 \times 10^{-2}$, $\hat{C} = 2$.

$$K_C = \frac{k_C}{k_R}, \; M_S = \frac{m_S}{m_W}, \; C_S = \frac{c_S}{c_R}, \; K_S = \frac{k_S}{k_R}, \text{ and } \hat{C} = \frac{C}{\varepsilon}$$

It should be noted that using the transformation $\bar{r}(t) = \bar{\rho}(t)e^{i\omega t}$ Equations (3) and (6) can also be presented in a rotating coordinates frame.

Figure 3 shows, in rotating coordinates, the rotor's response to full annular rub without considering the thermal effect, that is, for $p = 0$, and for the rotor's running speed just below the critical speed, that is, for $\omega = 0.95\omega_R$. Also, the contact force is nonlinear with the exponent $n = 1.5$ (see Equation (2)). The computed response clearly indicates transient behavior.

Figure 4 presents the rotor response for the same operating conditions as Figure 3, except that now the parameter representing the heat input to the rotor does have nonzero value, that is, $p = 1.51$. It can be seen that after initial transient behavior, the rotor starts to exhibit unstable spiral vibrations with a growing amplitude and phase angle (which can be seen only in a rotating coordinates frame). The spiral is traced out against the shaft's rotation.

STATE-SPACE REPRESENTATION OF THE MULTIMASS ROTOR/SEAL DYNAMICS

For the multimass rotor-bearing model limited to lateral vibrations, the matrix equation of motion (in stationary coordinates) can be written as follows:

$$\mathbf{M}\ddot{\mathbf{x}} + \mathbf{D}\dot{\mathbf{x}} + \mathbf{K}\mathbf{x} = \mathbf{f}(t) \qquad [9]$$

where $\mathbf{x}$ is $(n \times 1)$ the vibration vector; $\mathbf{M}$, $\mathbf{D}$, and $\mathbf{K}$, are $(n \times n)$ mass, damping, and stiffness matrices, respectively; and $\mathbf{f}(t)$

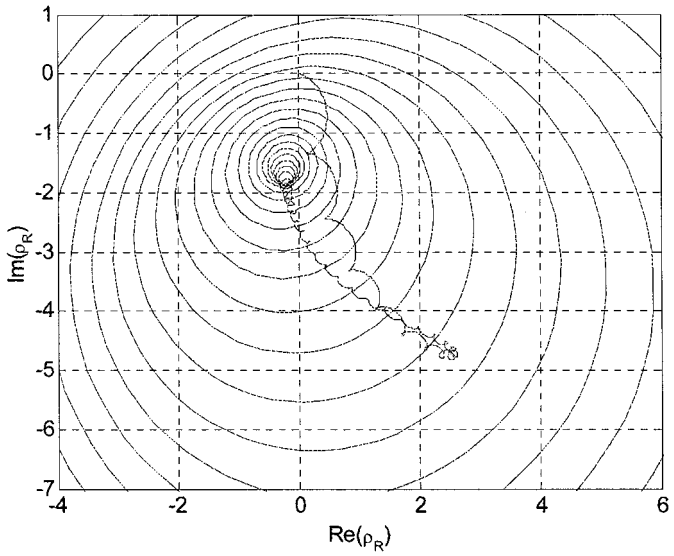

FIGURE 4
Rotor response, in rotating coordinates, to rub, with thermal effects. $\eta = 0.95$, $p = 1.51$, $q = 1 \times 10^{-3}$, $\xi_R = 0.05$, $M_S = 1 \times 10^{-5}$, $C_S = 0.7$, $K_S = 200$, $\mu = 0.2$, $K_C = 1 \times 10^{-2}$, $\hat{C} = 1.5$.

is the excitation force vector. The properties of bearings are included in matrices **D** and **K**.

The equation of motion for the multimass rotor-bearing system with thermal bow takes the following form (Schmied, 1987):

$$\mathbf{M}\ddot{\mathbf{x}} + \mathbf{D}\dot{\mathbf{x}} + \mathbf{K}\mathbf{x} - \mathbf{K}^R\mathbf{T}\mathbf{x}_{Ths} = \mathbf{f}(t) \qquad [10]$$

where $\mathbf{K}^R$ is $(n \times n)$ the stiffness matrix of the rotor without pedestals and bearings; **T** is the $(n \times 2)$ matrix describing the linear relation between the thermal deflections of all coordinates and the translatory coordinates at the rubbing site (the hot spot); and $\mathbf{x}_{Ths}$ is (2×1) the vector of thermally induced translatory displacements at the location of the hot spot (rubbing).

In stationary coordinates, the thermal equation can be written in the following form (Kellenberger, 1980):

$$\mathbf{I}\dot{\mathbf{x}}_{Ths} + \mathbf{P}\mathbf{x}_{hs} + \mathbf{Q}\mathbf{x}_{Ths} = \mathbf{0} \qquad [11]$$

where **I** and **0** are (2×2) unity and zero matrices, respectively, and $\mathbf{x}_{hs}$ is the (2×1) vector of translatory displacements of the shaft at the location of the rubbing. The matrices **P** and **Q** are (2×2) and represent added heat and dissipated heat, respectively.

Equations (10) and (11) are coupled and can be combined as follows:

$$\begin{bmatrix} \mathbf{M} & \mathbf{0} \\ \mathbf{0} & \mathbf{0} \end{bmatrix} \begin{Bmatrix} \ddot{\mathbf{x}} \\ \ddot{\mathbf{x}}_{Ths} \end{Bmatrix} + \begin{bmatrix} \mathbf{D} & \mathbf{0} \\ \mathbf{0} & \mathbf{I} \end{bmatrix} \begin{Bmatrix} \dot{\mathbf{x}} \\ \dot{\mathbf{x}}_{Ths} \end{Bmatrix} + \begin{bmatrix} \mathbf{K} & -\mathbf{K}^R\mathbf{T} \\ \bar{\mathbf{P}} & \mathbf{Q} \end{bmatrix} \begin{Bmatrix} \mathbf{x} \\ \mathbf{x}_{Ths} \end{Bmatrix} = \begin{Bmatrix} \mathbf{f}(t) \\ \mathbf{0} \end{Bmatrix} \qquad [12]$$

where $\bar{\mathbf{P}}$ is $(2 \times n)$ a matrix having coefficients of matrix **P** at the columns corresponding to the translatory coordinates $\mathbf{x}_{hs}$ of the hot spot.

Introducing state variables, defined as $\mathbf{x}_1 = \mathbf{x}$, $\mathbf{x}_2 = \dot{\mathbf{x}}$, $\mathbf{x}_3 = \mathbf{x}_{Ths}$, and writing the equations

$$\begin{cases} \dot{\mathbf{x}}_1 = \mathbf{x}_2 \\ \mathbf{M}\dot{\mathbf{x}}_2 = -\mathbf{K}\mathbf{x}_1 - \mathbf{D}\mathbf{x}_2 + \mathbf{K}^R\mathbf{T}\mathbf{x}_3 + \mathbf{f} \\ \dot{\mathbf{x}}_3 = -\bar{\mathbf{P}}\mathbf{x}_1 - \mathbf{Q}\mathbf{x}_3 \end{cases} \qquad [13]$$

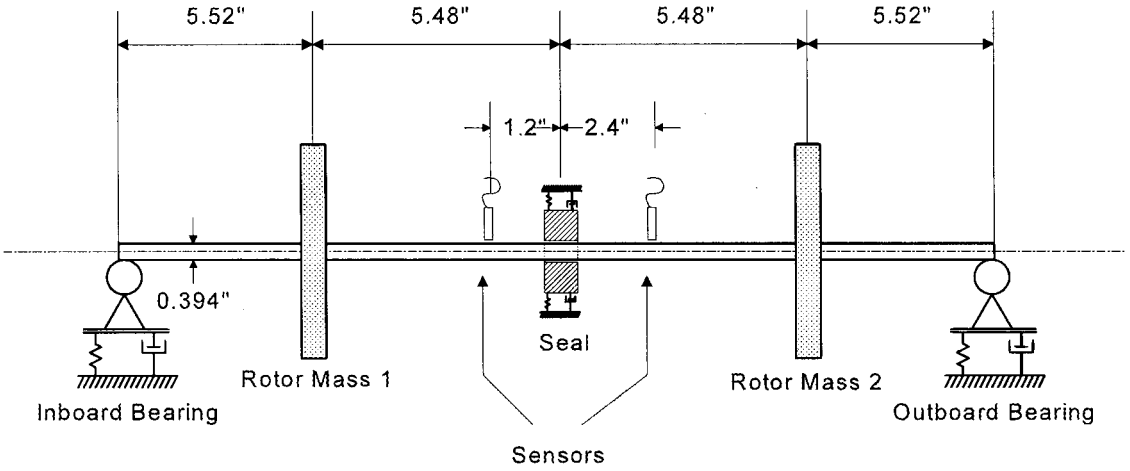

FIGURE 5
Diagram of rotor/seal test rig with two disks.

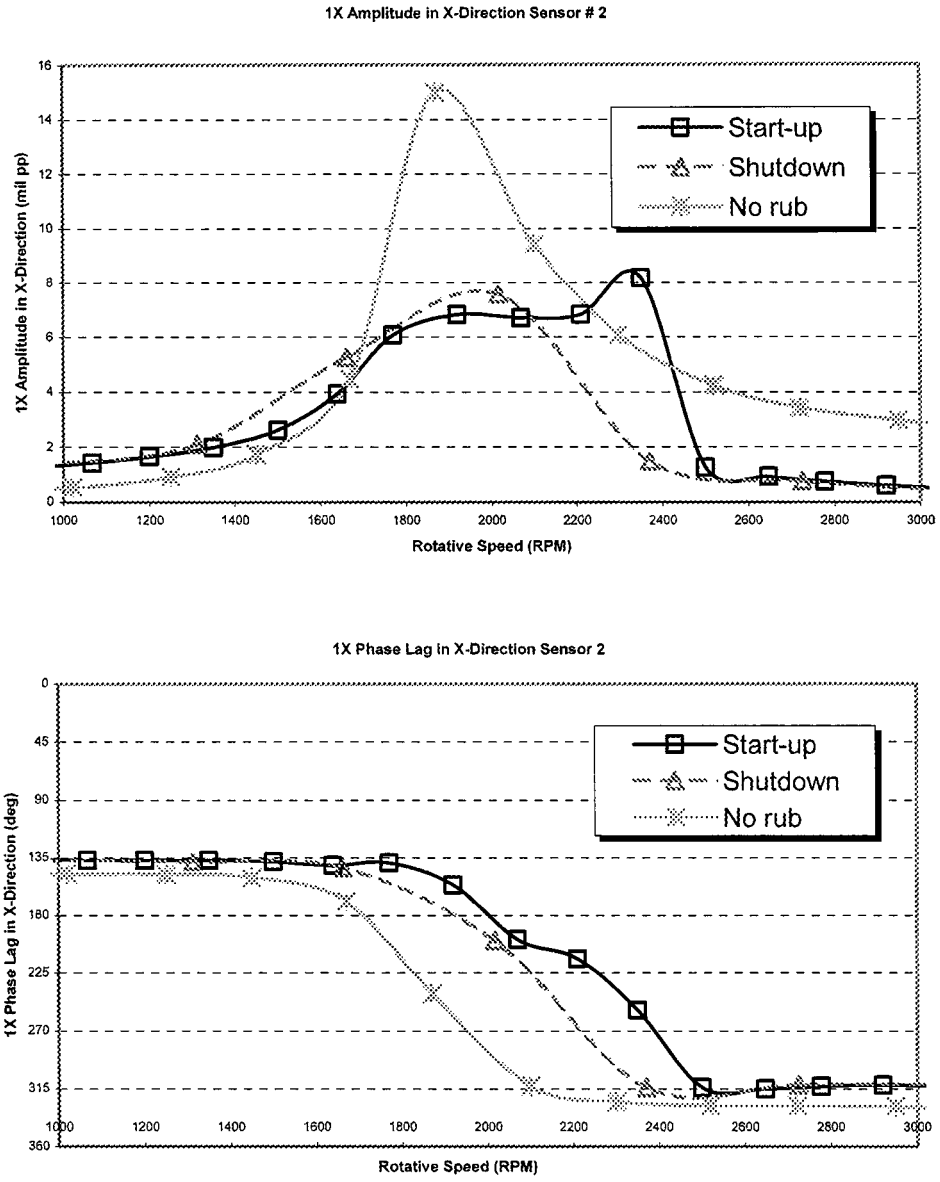

FIGURE 6
Responses (1×) of the two-disk rotor during start-up and shutdown, testing both with and without rubbing.

allows the state equation to be written as follows:

$$\dot{\mathbf{x}} = \mathbf{A}\mathbf{x} + \mathbf{B}\mathbf{u} = \begin{bmatrix} \mathbf{0} & \mathbf{I} & \mathbf{0} \\ -\mathbf{M}^{-1}\mathbf{K} & -\mathbf{M}^{-1}\mathbf{D} & \mathbf{M}^{-1}\mathbf{K}^{R}\mathbf{T} \\ -\bar{\mathbf{P}} & \mathbf{0} & -\mathbf{Q} \end{bmatrix} \cdot \mathbf{x} + \begin{bmatrix} \mathbf{0} \\ \mathbf{M}^{-1} \\ \mathbf{0} \end{bmatrix} \mathbf{f} \quad [14]$$

where the state vector is defined as $\mathbf{x} = (\mathbf{x}_1, \mathbf{x}_2, \mathbf{x}_3)^T$. The stability of the system (Equation (12)) can be conveniently determined by analysis of the real part of the eigenvalues of state matrix **A**.

EXPERIMENTAL STUDY RESULTS

Full annular rub in a rotor/seal system was investigated experimentally. A shaft with a diameter of 0.394 inches and a length of 22 inches was supported by two brass bearings and driven by a 0.1-hp motor. Two disks were attached as is shown in Figure 5. A seal was located at the midspan. The bronze seal used in the experiment was fitted with an O-ring in the seal support and had 6 mils of diametral clearance. The rotor was originally centered in the seal and well balanced. A known mass unbalance (4.4×10^{-4} lbm) was then added to each disk. Without contact with the seal, the rotor's initial, balanced resonance speed was approximately 1850 rpm. The data acquisition and processing system consisted of four XY displacement proximity probes (Figure 5),

one speed probe, one Keyphasor probe to measure speed and phase, and ADRE software.

The $1\times$ Bode plots of the X-direction responses of the two-disk rotor during the startup and shutdown testing, with and without rubbing, are presented in Figure 6. In the test with the rubbing, the peak amplitude of vibration was limited by the clearance between the rotor and the seal. In addition, the inherent nonlinearity of the system gave rise not only to subharmonic vibrations (Sawicki et al., 1999), but also to amplitude jump discontinuities, which occur when multitude solutions exist. This is clearly demonstrated in Figure 6. It is mainly during the startup that the amplitude drops down; then it jumps up during the shutdown operation. The range of resonance speeds is much wider during startup than it is during shutdown.

An excellent description of the phenomena observed was provided by Bently and colleagues (2000a, 2000b), who presented insightful data concerning the experiment and studied the precessional rub in great detail. They also analyzed the effect of unbalance, friction, rotative speed, rub frequency, and other parameters.

SUMMARY AND CONCLUSIONS

Rubbing occurring in a rotor/stator/seal system was investigated analytically, numerically, and experimentally. The analytical model accounts for the thermal effect associated with rubbing. The characteristic spiral vibrations of the generic rotor/stator system was calculated. The issue of the stability of multimass rotor-bearing systems subjected to thermal bow due to the occurrence of rub was addressed by developing a procedure based on the state-space representation and eigenvalue analysis. Finally, the characteristic for full annular rub amplitude jump has been demonstrated experimentally.

NOMENCLATURE

S	Geometric center of the stator
R	Geometric center of the rotor (also radius of the rotor)
G	Rotor center of gravity
ε	Mass eccentricity
m_R	Rotor mass
k_R	Rotor stiffness
c_R	Rotor damping
m_S	Stator mass
k_S	Stator stiffness
c_S	Stator damping
r_T	Thermal bow in inertial coordinates frame
ω	Angular speed of rotor
ω_R	Rotor critical speed
$\bar{F}_R$	Contact force vector
μ	Coulomb friction coefficient
k_C	Contact stiffness between rotor and stator
C	Concentric radial clearance
γ	Position of the hot spot
ξ_R	Rotor damping ratio
$\bar{r}_R$	Rotor vibration vector in inertial coordinates frame
$\bar{\rho}_R$	Rotor vibration vector in rotating coordinates frame
T	Excess temperature
Q_1	Heat entering the rotor per unit time
Q_2	Heat loss per unit time

REFERENCES

Bently, D. E. 1974. Forced subrotative dynamic action of rotating machinery. ASME Publication, 74-Pet-16, *Petroleum Mechanical Engineering Conference*, Dallas, TX.

Bently, D. E., Goldman, P., and Yu, J. J. 2000. Full annular rub in mechanical seals Part II: Analytical study. *Proceedings of the 8th International Symposium on Transport Phenomena and Dynamics of Rotating Machinery, ISROMAC-8*, Honolulu, HI, pp. 1003–1010.

Bently, D. E., Goldman, P., and Yu, J. J. 2000. Full annular rub in mechanical seals Part I: Experimental results, *Proceedings of the 8th International Symposium on Transport Phenomena and Dynamics of Rotating Machinery, ISROMAC-8*, Honolulu, HI, pp. 995–1002.

Childs, D. W. 1997. Clearance effects on spiral vibrations due to rubbing. *Proceedings of the 1997 ASME Design Engineering Conferences, DETC-97*, 16th Biennial Conference on Mechanical Vibration and Noise, Sacramento, CA, pp. 1–9.

Dimarogonas, A. D. 1973. Newkirk effect, thermally induced dynamic instability of high-speed rotors. International Gas Turbine Conference, Washington, DC. ASME Paper No. 73-GT-26.

Dimarogonas, A. D. 1983. *Analytical Methods in Rotor Dynamics*. London: Applied Science Publishers.

Ehrich, F. 1992. Observations of subcritical superharmonic and chaotic response in rotordynamics. *ASME Journal of Vibration and Acoustics* 114:93–100.

Goldman, P., and Muszynska, A. 1993. Chaotic behavior of rotor/stator systems with rubs. *ASME Turbo Expo Conference*, Cincinnati.

Goldman, P., and Muszynska, A. 1994. Dynamic effects in mechanical structures with gaps and impacting: Order and chaos. *ASME Journal of Vibration and Acoustics* 116:541–547.

Kellenberger, W. 1980. Spiral vibrations due to seal rings in turbogenerators: Thermally induced interaction between rotor and stator. *ASME Journal of Mechanical Design* 102:177–184.

Kirk, R. G., and Balbahadur, A. C. 2000. Thermal distortion synchronous rotor instability. *Proceedings of the 7th International Conference on Vibrations in Rotating Machinery*, ImechE, Paper C576/041, pp. 427–436, Nottingham, UK.

Kraker, D., Crooijmans, M. T. M., and Campen, D. H. 1988. The dynamics of a rotor with rubbing. *Proceedings of the 4th International Conference on Vibrations in Rotating Machinery*, ImechE, Paper C284/88, pp. 297–303, Edinburgh, UK.

Liebich, R. 1998. Rub induced non-linear vibrations considering the thermo-elastic effect. *Proceedings of the Fifth International Conference on Rotor Dynamics*, IFToMM, 802-815, Darmstadt, Germany.

Muszynska, A. 1989. Rotor-to-stator element rub-related vibration phenomena in rotating machinery—literature survey. *Shock and Vibration Digest* 21(3):3–11.

Newkirk, B. L. 1926. Shaft rubbing: Relative freedom of rotor shafts from sensitiveness to rubbing contact when running above their critical speeds. *Mechanical Engineering* 48(8):830–832.

Padovan, J., and Choy, F. K. 1987. Nonlinear dynamics of rotor/blade/casing rub interactions. *ASME Journal of Turbomachinery* 108:527–534.

Sawicki, J. T., Padovan, J., and Al-Khatib, R. 1999. The dynamics of rotor with rubbing. *International Journal of Rotating Machinery* 5(4):295–304.

Sawicki, J. T. 2000. Steam turbine rotors rub sensitivity study. Phase I: The development study. Technical report submitted to GE Corporate Research & Development Center, Schenectady, NY.

Schmied, J. 1987. Spiral vibrations of rotors. *Proceedings of the 11th Biennial ASME Vibration and Noise Conference.* Boston, pp. 449–456.

Taylor, H. D. 1924. *Rubbing Shafts Above and Below the Resonance Speed (Critical Speed)*, General Electric Company, R-16709, Schenectady, NY.